*Biochimica et Biophysica Acta* 807 (1985) 101–109
Elsevier



BBA 41722

# Magnetophotoselection of *Rhodopseudomonas sphaeroides* wild-type reaction centers

William J. McGann and Harry A. Frank

*Department of Chemistry, Box U-60, University of Connecticut, Storrs, CT 06268 (U S A )*

(Received August 7th, 1984)

Key words Magnetophotoselection; Reaction center, ESR; Pigment orientation; Triplet state; (*Rps sphaeroides*)

**Chemically reduced reaction centers of the photosynthetic bacteria *Rhodopseudomonas sphaeroides* wild type give rise to carotenoid triplet-state electron spin resonance signals upon illumination at 85 K. The relative signal intensities are found to depend on both the wavelength and the polarization of the excitation. These data are used to calculate the orientations of the primary donor 870 nm transition moment and the carotenoid 514 nm transition moment with respect to each other and with respect to the carotenoid principal magnetic axis system. The angle between the primary donor and the carotenoid transition moments is found to be $75 \pm 8°$ and taken together with data published previously (Frank, H.A., Bolt, J., Friesner, R. and Sauer, K. (1979) Biochim. Biophys. Acta 547, 502–511 and Frank, H.A., Machnicki, J.P. and Toppo, P. (1984) Photochem. Photobiol. 39, 429–432) is used to calculate the orientation between primary donor and the carotenoid principal magnetic-axis systems.**

## Introduction

Magnetophotoselection is a technique which combines the optical photoselection and the triplet state electron spin resonance (ESR) experiments [1]. The method is carried out by exciting a randomly distributed sample with polarized light and recording the light-induced ESR spectrum with the excitation polarization parallel and perpendicular to the static ESR field. Kottis and Lefebvre [2] first suggested that magnetophotoselection be used to study the orientation of donor-acceptor pairs in triplet–triplet energy-transfer processes. Since then the technique has been used to study triplet energy transfer between aromatic molecules [3–6] and also to assign the directions of the principal magnetic axes of photoexcited triplet states in several aromatic systems [6–10], including the chlorophylls [11].

Magnetophotoselection [12–15] and optical photoselection [16–20] have both been used to study the relative orientations of the chromophores contained in bacterial photosynthetic reaction center proteins. Thurnauer et al. [12] used magnetophotoselection to determine the orientation of the primary donor transition moments with respect to the primary donor principal magnetic axis system in $K_2IrCl_6$-treated chromatophores of *Rhodospirillum rubrum*. Their results were that the primary donor transition moment lay along the $x$ magnetic axis in the primary donor triplet state spectrum. Frank et al. [13] determined, in a magnetophotoselection study of *Rhodopseudomonas sphaeroides* R26 reaction centers, the orientations of the primary donor and one of the reaction center bacteriopheophytin molecules in the principal magnetic-axis system of the primary donor. Their work showed that the primary donor transi-

Abbreviations: LDAO, lauryldimethylamine *N*-oxide; DEAE, diethylaminoethyl

tion moment was oriented 8° from the $x$ magnetic axis, 89° from the $y$ magnetic axis and 82° from the $z$ magnetic axis of the primary donor triplet. The authors further showed that the primary donor transition moment at 870 nm makes an angle of 60° with respect to the bacteriopheophytin transition moment at 546 nm. At approximately the same time, Boxer and Roelofs [15] determined in a magnetophotoselection study the orientation between the bacteriopheophytin transition moments at 535 and 546 nm. Their data showed that the angle between the bacteriopheophytin transition moments was $86 \pm 2°$. This was in agreement with the linear dichroism data presented by Clayton et al. [20].

Prior to the magnetophotoselection studies of Frank et al. [13] and Boxer and Roelofs [15], Vermeglio et al. [16] performed optical photoselection studies on reaction centers of *Rps. sphaeroides* wild type to determine the orientations of several transition moments relative to the primary donor transition moment. One of their conclusions was that the angle between the bacteriopheophytin absorbing at 546 nm and the primary donor transition moments is approx. 60° (in agreement with Frank et al. [13]), and the angle between the carotenoid and the primary donor transition moments is greater than or equal to 72°. There were two reasons for their reporting the latter angle as a lower limit. First, because of depolarization effects in the optical photoselection spectra, the authors had to correct their polarization values in the carotenoid absorption region to account for the excitation of other transition moments. Second, the polarization ratio expression is less sensitive a probe of the angle between transition moments as the angle approaches 90°, leading to more uncertainty in the determination [21].

By orienting *Rps. sphaeroides* wild-type chromatophores on mylar strips, Frank et al. [22] were able to use ESR to determine the orientations of the primary donor magnetic axes and the carotenoid magnetic axes with respect to the membrane normal. The explicit orientation between the primary donor and the carotenoid magnetic axis systems could not be specified because the determination yielded projections of the magnetic axes onto the normal to the membrane, and not projections of one axis system onto the other. The orientation of the carotenoid transition moment in the carotenoid principal magnetic axis system is needed to specify the orientation between the two magnetic axis systems (see below).

In this paper we present magnetophotoselection experiments on reaction centers of *Rps. sphaeroides* wild type. The goals of this work are: (i) to determine the orientations of the carotenoid and the primary donor transition moments in the carotenoid principal magnetic axis system, (ii) to determine the precise value of the angle between the primary donor and carotenoid transition moments, and (iii) to determine the orientation between the primary donor and the carotenoid principal magnetic axes systems.

The orientation of the carotenoid transition moment in the carotenoid principal magnetic axis system is calculated by computer simulations of the observed triplet state spectra according to the procedure of Frank et al. [13,23]. The approach is to use Eqn. 1 for the triplet state ESR spectral intensity to simulate the experimental ESR lineshape:

$$\bar{I}(|\mathbf{H}|) = \int_0^{\pi}\int_0^{2\pi} I(\theta, \phi, |\mathbf{H}|) D_i(\theta, \phi) \mathrm{d}\theta \mathrm{d}\phi$$

$$i = r, \|, \perp \tag{1}$$

where $\bar{I}(|\mathbf{H}|)$ is the signal intensity at field $|\mathbf{H}|$ whose orientation in the magnetic axis system is specified by the polar angles $\theta$ and $\phi$. $D_i(\theta, \phi)$ are the distribution functions which describe the probability that a member of the ensemble has a static field direction given by $\theta$ and $\phi$. These distribution functions have been derived previously [13] and are:

$$D_r(\theta, \phi) = \sin\theta \tag{2}$$

$$D_{\|}(\theta, \phi) = (P_1 \cos\theta + P_2 \sin\theta \cos\phi + P_3 \sin\theta \sin\phi)^2 \sin\theta \tag{3}$$

$$D_{\perp}(\theta, \phi) = \tfrac{1}{2}\left[1 - (P_1 \cos\theta + P_2 \sin\theta \cos\phi + P_3 \sin\theta \sin\phi)^2\right] \sin\theta \tag{4}$$

where $D_r(\theta, \phi)$ is the distribution function describing the random ensemble, and $D_{\|}(\theta, \phi)$ and $D_{\perp}(\theta, \phi)$ describe the ensemble distributions gen-

erated by light polarized parallel and perpendicular to the static ESR field respectively. $P_1$, $P_2$ and $P_3$ are the projections of the excited transition moment onto the carotenoid magnetic axes. The magnetophotoselection spectra are simulated using Eqn. 1 with $P_1$, $P_2$ and $P_3$ as parameters. Once the spectrum is calculated and the projections are known, the angle between the carotenoid and the primary donor transition moments can be determined from the scalar product of the transition moments (see below). Then using data on the orientation of the primary donor transition moment in the primary donor principal magnetic axis system [13] and the orientation of the principal magnetic axes of the primary donor and the carotenoid with respect to the normal to the membrane [22], the explicit orientation between the carotenoid and the primary donor principal magnetic axis systems in the photosynthetic membrane can be calculated.

## Materials and Methods

*Rps. sphaeroides* wild type cells were grown anaerobically in a 3% yeast extract/3% bactopeptone media. Reaction centers were prepared in the following way. Chromatophores were obtained by french pressure disruption at $1.4 \cdot 10^8$ Pa of whole cells followed by ultracentrifugation at $150\,000 \times g$ for 90 min. The chromatophore membranes were solubilized by incubation in a 0.3% LDAO (lauryldimethylamine *N*-oxide)/10 mM Tris buffer (pH 8.0) at 22°C for 15 min. The mixture was then centrifuged at $15\,000 \times g$ for 10 min to remove the membrane debris. The supernatant was then loaded onto a DEAE sephacel (anion exchange) column (135 ml bed volume) which was previously equilibrated with 0.1% LDAO/10 mM Tris buffer (pH 8.0). The protein fractions were eluted from the column by a step gradient elution using 0.15–0.20 M NaCl/10 mM Tris buffer (pH 8.0) solutions. The elution was carried out in 0.01 M NaCl concentration steps. The reaction center protein fractions were obtained at 0.18 M NaCl concentration. The reaction center proteins were dialyzed against 10 mM Tris buffer (pH 8.0) and concentrated by dialysis against solid sucrose. The concentrated fraction (absorbance 2.5 at 800 nm) was loaded onto a DEAE sephacel column (10 ml bed volume) to remove free pigments. The purified reaction centers were obtained by elution with 0.5 M NaCl/10 mM Tris buffer (pH 8.0).

Reaction center samples to be used in the ESR experiments were prepared in the following way. The samples were deoxygenated by bubbling with $N_2$ gas (5 min) and chemically reduced by the addition of sodium dithionite ($Na_2S_2O_7$) to a final concentration of 100 mM. An equal volume of deoxygenated ethylene glycol (Fisher) was added to ensure that a clear glassy sample was obtained upon freezing. The sample mixture was placed in a quartz ESR tube (3 mm inside diameter × 4 mm outside diameter), capped and frozen slowly in liquid nitrogen to prevent sample cracking.

Triplet state ESR spectroscopy was carried out using a Varian X-band spectrometer. The magnetic field modulation amplitude and frequency were 25 G and 100 kHz, respectively. Excitation into the carotenoid absorption bands was accomplished with an argon ion laser (Spectra-Physics model 164) at 514 nm. The laser light was defocussed by a plano-convex lens to a beam diameter of 1 cm. The beam polarization was rotated using an half wave plate in tandem with a prism polarizer. Excitation into the primary donor absorption bands at 870 nm was accomplished by using a 1000 W xenon arc lamp (Kratos LH 151N/1S). Selective excitation into the 870 nm absorption band was accomplished by a series of Schott glass cutoff filters (RG-550, RG-630, RG-710 and RG-850) in tandem with a $K_2SO_4/Cr_2(SO_4)_3$ 24 $H_2O$ solution filter (3.5 cm path). The magnetophotoselection effects obtained using 870 nm excitation in this configuration were reproduced using an 880 nm interference filter (Ealing 35-4555). Polarization of the xenon source was achieved by a Polaroid type HN-7 sheet polarizer. The extent of depolarization of the source as measured by the light transmission through two HN-7 polarizers with their transmission axes crossed was less than 5% at 870 nm.

In all the ESR experiments, the light was amplitude modulated at 44 Hz and focussed onto a Varian TE microwave cavity fitted with an open ended flange to allow 100% transmission of the exciting light. The light-induced signals were phase detected using a lockin amplifier (PAR model 128A) referenced to the light chopper. The sample

temperature in all experiments was 85 K unless otherwise stated.

## Results

Fig. 1 shows the ESR spectrum of chemically reduced *Rps. sphaeroides* wild-type reaction centers. This spectrum was generated at a sample temperature of 85 K using broadband visible illumination. Fig. 2 displays the carotenoid triplet state ESR spectra generated by 514 nm excitation which excites directly into the carotenoid absorption region. The excitation was polarized parallel (Fig. 2a) and perpendicular (Fig. 2b) to the static ESR field direction. Fig. 3 displays the carotenoid triplet state spectra generated by 870 nm excitation which excites the primary donor bacteriochlorophyll. Again, the excitation was polarized parallel (Fig. 3a) and perpendicular (Fig. 3b) to the static field direction.

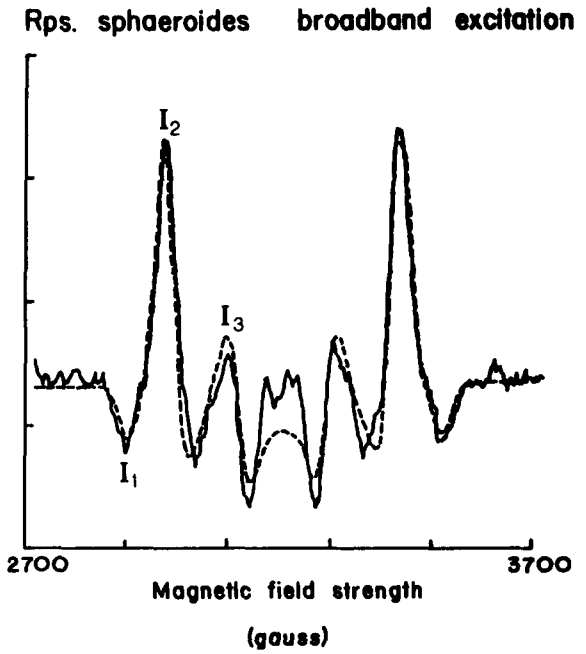


Fig. 1. Carotenoid triplet state ESR spectrum of *Rps sphaeroides* wild-type reaction centers. The solid line denotes the experimental spectrum taken under the following conditions: temperature, 85 K; modulation amplitude, 25 G, microwave frequency, 9.054 GHz; microwave power, 16 mW; light modulation frequency, 44 Hz, lockin amplifier sensitivity, 1 mV sweep rate, 50 G/min; recorder time constant, 10 s. The dashed line represents the computer-generated spectrum. The simulation conditions are given in Table I.

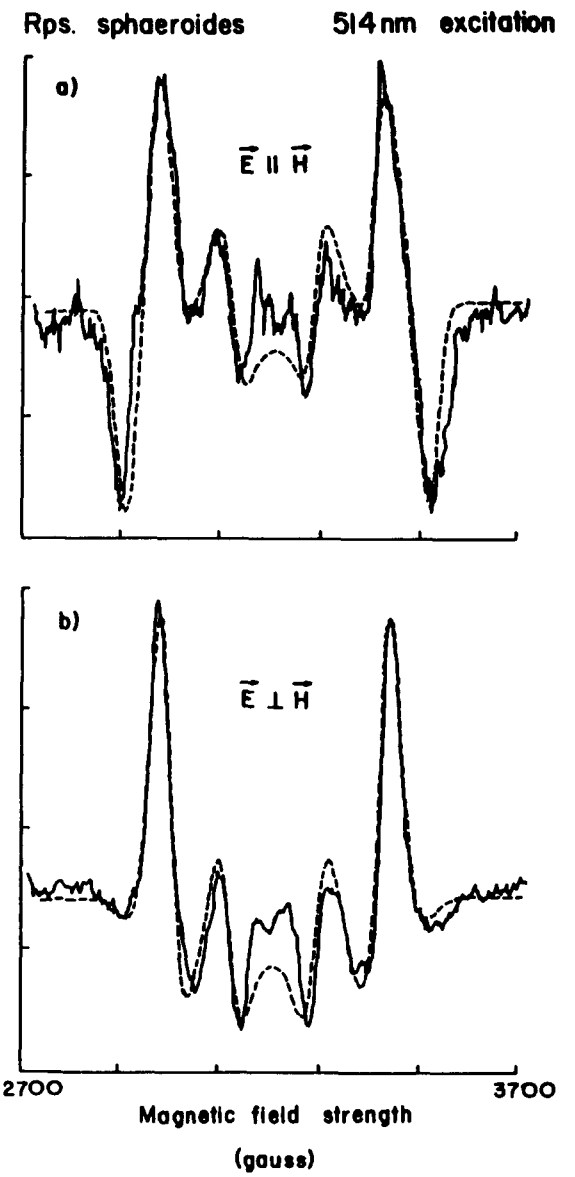


Fig. 2. Carotenoid triplet state ESR spectrum of *Rps sphaeroides* wild-type reaction centers upon excitation into the carotenoid absorption band at 514 nm. The solid lines represent the experimental spectra taken with the laser source polarized parallel ($E \| H$) and perpendicular ($E \perp H$) to the static ESR magnetic field direction. The experimental conditions were the same as those stated in Fig 1 with the following exceptions: (a) laser power, 1.0 W defocussed, lockin amplifier sensitivity, 250 $\mu$V, sweep rate, 25 G/min, recorder time constant, 30 s. (b) laser power 1 0 W defocussed; lockin amplifier sensitivity, 1 mV; sweep rate, 25 G/min; recorder time constant, 30 s. The dashed lines denote the computer-generated spectra. The simulation parameters were the same as those used to simulate Fig. 1 in addition to the projections of the carotenoid transition moment onto the carotenoid principal magnetic axes given in Table II.

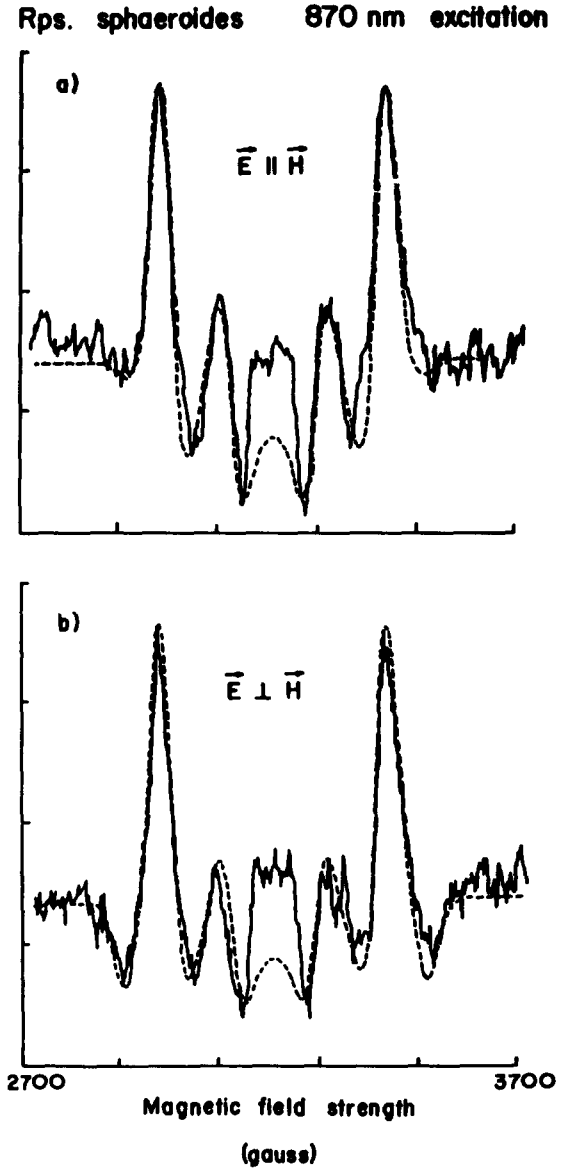


Fig. 3. Carotenoid triplet state ESR spectrum of *Rps. sphaeroides* wild-type reaction centers upon excitation of the primary donor at 870 nm. The solid lines represent the experimental spectra taken under the experimental conditions in Fig. 1 except: sweep rate, 25 G/min; recorder time constant, 30 s. The dashed lines denote the computer-generated spectra. The simulation parameters were the same as those used to simulate Fig. 1 in addition to the projections of the primary donor transition moment onto the carotenoid principal magnetic axes given in Table II.

Computer simulations of the experimental ESR spectra (Figs. 1–3; dashed lines) were achieved using Eqn. 1 in conjunction with an appropriate distribution function (Eqns. 2–4). The simulations were accomplished as follows. First, Eqns. 1 and 2 were used to calculate the broadband spectrum. This was done by initially approximating the zero-field splitting parameters, $|D|$ and $|E|$, from the experimental splittings [22]. The $|D|$ and $|E|$ values then were varied until the field positions of the calculated spectrum matched the experimental field positions. Then the depopulation rate constants for triplet decay were varied until the calculated intensities at the resonance field positions matched the experimental intensities [23]. Finally, the intrinsic linewidth parameter was varied until the linewidths of the calculated spectral peaks matched those of the experimental spectrum.

The spectra taken using polarized light were

TABLE I

ZERO-FIELD SPLITTING PARAMETERS, TRIPLET-STATE DEPOPULATION RATE CONSTANTS, AND INTRINSIC LINEWIDTH, USED IN THE COMPUTER SIMULATION OF THE RANDOM SPECTRUM OF *RPS SPHAEROIDES* WILD TYPE

$|D|$ and $|E|$ are the zero-field splitting parameters, $k_1$, $k_2$ and $k_3$ are the depopulation rate constants of the triplet spin sublevels associated with the $I_1$, $I_2$ and $I_3$ signal intensities in Fig. 1, and $\delta$ is the intrinsic linewidth parameter.

| | |
|---|---|
| $\|D\|$ | $0.0286 \pm 0.0006$ cm$^{-1}$ |
| $\|E\|$ | $0.0044 \pm 0.0003$ cm$^{-1}$ |
| $k_1$ | $12500 \pm 1000$ s$^{-1}$ |
| $k_2$ | $4500 \pm 500$ s$^{-1}$ |
| $k_3$ | $9000 \pm 1000$ s$^{-1}$ |
| $\delta$ | $26.0 \pm 3.0$ G |

TABLE II

PROJECTIONS OF THE OPTICAL TRANSITION MOMENTS AT 514 AND 870 nm ONTO THE PRINCIPAL MAGNETIC AXES OF THE CAROTENOID TRIPLET STATE

$P_1$, $P_2$ and $P_3$ are the projections of the optical transition moment onto the carotenoid principal magnetic axes labelled 1, 2 and 3 in Fig. 4

| Transition moment | $P_1$ | $P_2$ | $P_3$ |
|---|---|---|---|
| 514 nm (carotenoid) | $0.82 \pm 0.03$ | $0.37 \pm 0.03$ | $0.42 \pm 0.02$ |
| 870 nm (primary donor) | $0.32 \pm 0.08$ | $0.72 \pm 0.08$ | $0.60 \pm 0.07$ |

simulated using the distribution functions given in Eqns. 3 and 4. The projections of the optical transition moment onto the principal magnetic axes $P_1$, $P_2$ and $P_3$ were varied until the calculated spectral intensities matched those of the experimental spectrum. The simulation parameters for the spectra presented in Figs. 1–3 are summarized in Tables I and II.

## Discussion

As stated in the introduction, magnetophotoselection can be used to determine the orientation of an optical transition moment in a principal magnetic axis system. In the present study, the projections of the carotenoid and the primary donor transition moments have been specified with respect to the principal magnetic axes of the carotenoid triplet (see Table II). These results make it possible to determine the angle between the transition moments. This angle, denoted $\gamma$, between the carotenoid transition moment, $\mu_{514}$, and the primary donor transition moment, $\mu_{870}$, is calculated from the arccosine of the dot product of the transition moment vectors; viz.:

$$\gamma = \arccos|\mu_{514}\ \mu_{870}| \tag{5}$$

Because the sign of the projections of the transition moment in the principal axis system is indeterminate in a magnetophotoselection experiment, all possible sign combinations of the projections must be considered in Eqn. 5. i.e.:

$$|\mu_{514}\ \mu_{870}| = |\pm P_1P_1' \pm P_2P_2' \pm P_3P_3'| \tag{6}$$

where the $P$ values specify the projections of the transition moments in the carotenoid magnetic axis system. As a result, two regions of solution for $\gamma$ are obtained using the projections given in Table II. These regions are $\gamma = 37 \pm 4°$ and $\gamma = 75 \pm 8°$. The first region of solution, $\gamma = 37 \pm 4°$, is not consistent with the optical photoselection data of Vermeglio et al. [16]. These authors monitored the actinic light-induced change in absorption at 870 nm with the detector polarized parallel and perpendicular to the direction of the polarized excitation. Their conclusion was that the carotenoid transition moment makes an angle of greater than or equal to 72° with the primary donor transition moment. As stated in the introduction, the value is reported as a lower limit because of depolarization effects in the carotenoid absorption region and the fact that polarization ratio expression is less sensitive a probe of $\gamma$ as the angle approaches 90°. Their polarization values were corrected for depolarization effects resulting from excitation of other transition moments in the carotenoid absorption region of the spectrum.

Depolarization effects in the magnetophotoselection experiment would reduce the differences in the peak intensities between spectra taken in the parallel and perpendicular orientations and tend to randomize the observed spectra. In the case of the spectra generated by excitation into the carotenoid absorption band at 514 nm (Fig. 2) the largest magnetophotoselection effect is observed in the outermost peaks. Because depolarization would tend to minimize the differences in the intensities of these and the other peaks in the parallel and perpendicular spectra, the extent of depolarization in the present experiments can be determined. It is limited to a value proportional to the ratio of the intensity of the outermost feature in the perpendicular spectrum to the corresponding feature in the parallel spectrum. This value is approx. 0.1. Assuming that all of the intensity in the outermost peak in the perpendicular spectrum arises from depolarization effects, the value for the projection, $P_1$, along the magnetic axis (labelled 1 in Fig. 4). corresponding to these peaks would be calculated to be lower than the true value. The maximum theoretical value for $P_1$ is 1.00. This corresponds to the carotenoid transition moment being oriented directly along the this magnetic axis labelled (Fig. 4). Using this theoretical maximum value ($P_1 = 1.0$) in Eqn. 5, one obtains a value of 71° for $\gamma$ compared to the value of 75° calculated from the experimental results. Therefore, it is apparent that the effect of depolarization, although certainly present to some extent, is not a major factor in these determinations as the theoretical limit of $\gamma$ falls within the range of error based on the reproducibility of the experiment. Furthermore, the experimental spectra are simulated using a distribution function which includes the effect of exciting only one transition moment. Finally, because the end result must be consistent with the optical photo-

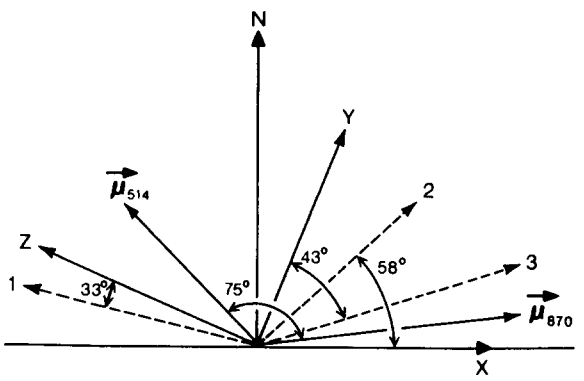


Fig 4. The orientations of the transition moments and the principal magnetic axis systems of the carotenoid and the primary donor $\mu_{514}$ and $\mu_{870}$ are the carotenoid and primary donor transition moments, respectively The axes labelled 1, 2 and 3 are the carotenoid magnetic axes corresponding to the peak intensities labelled $I_1$, $I_2$ and $I_3$, respectively in Fig. 1. The axes labelled $x$, $y$ and $z$ are the primary donor magnetic axes. $N$ is the normal to the membrane plane. The projections of the axes onto the normal to the membrane are drawn to correspond to the values reported in Ref. 22

selection experiments reported by Vermeglio et al. [16], the $\gamma = 37 \pm 4°$ solution is excluded, leaving the $\gamma = 75 \pm 8°$ solution as the angle between the two transition moments.

As a check on the value of $\gamma$, a second magnetophotoselection experiment was performed. By lowering the sample temperature from 85 K to 10 K, a temperature where the carotenoid triplet state no longer quenches the primary donor triplet [24], one can determine $\gamma$ using the primary donor principal magnetic axis system. The ESR spectra of the primary donor triplet state were obtained by exciting into the carotenoid absorption band at 514 nm using polarized excitation (spectra not shown). These experimental spectra were computer simulated to obtain the projections of the carotenoid transition moment onto the primary donor principal magnetic axes. The value of $\gamma$ was then determined using Eqn. 5 and along with the data of Frank et al. [13]. for the orientation of the primary donor transition moment in the principal magnetic axis system of the primary donor. Once again, two distinct regions of solution for $\gamma$ were calculated. These regions are $\gamma = 62 \pm 5°$ and $\gamma = 76 \pm 5°$. As before, the first region of solution, $\gamma = 62 \pm 5°$ can be excluded based on the optical photoselection results of Vermeglio et al. [16], which showed that $\gamma$ must be greater than or equal to 72°. The second region, $\gamma = 76 \pm 5°$ is within the experimental error of the previous determination, confirming its validity.

The problem of the orientation of the two magnetic axis systems is solved by first transforming the coordinates of the carotenoid transition moment from the carotenoid principal magnetic axis system into the primary donor principal magnetic axis system. This can be achieved by operating with the appropriate Euler angle transformation matrix on the vector to be transformed; viz.:

$$\mu'_{514} = \mathbf{M} \cdot \mu_{514} \tag{7}$$

$\mu'_{514}$ is the carotenoid transition moment having coordinates in the primary donor magnetic axis system. **M** is the Euler angle transformation matrix whose elements are the direction cosines of the angles between the primary donor and the carotenoid magnetic axes:

$$\mathbf{M} = \begin{pmatrix} \cos\theta_{11} & \cos\theta_{12} & \cos\theta_{13} \\ \cos\theta_{21} & \cos\theta_{22} & \cos\theta_{23} \\ \cos\theta_{31} & \cos\theta_{32} & \cos\theta_{33} \end{pmatrix} \tag{8}$$

where $\theta_{ij}$ is the angle between the $i$ magnetic axis of the primary donor and the $j$ magnetic axis of the carotenoid. Subtracting the carotenoid transition moment vector from the primary donor transition moment vector yields a resultant vector, $|\boldsymbol{R}|$, in the primary donor axis system;

$$|\boldsymbol{R}| = |\mu_{870} - \mu'_{514}| \tag{9}$$

$|\boldsymbol{R}|$ is also a function of $\gamma$, the angle between the two transition moments:

$$|\boldsymbol{R}| = 2 \sin\frac{\gamma}{2} \tag{10}$$

Equating these last two expressions yields an expression for $\gamma$ as a function of **M**:

$$\gamma = 2 \arcsin\frac{\mu_{870} - \mu'_{514}}{2} \tag{11}$$

Thus, the angle between the primary donor and the carotenoid transition moments ($75 \pm 8°$) can be used to determine the orientation of the primary

donor and the carotenoid magnetic axis systems. This is done in the following way. First, the orientation of the primary donor transition moment is specified in the primary donor magnetic axis system. As stated previously, the projections of the primary donor transition moment have been determined to be 0.99, 0.01, and 0.14 along the $x$, $y$, and $z$ magnetic axes of the primary donor, respectively [13]. Second, the orientation of the carotenoid transition moment must be specified within the carotenoid principal magnetic axis system. The values for the projections of the carotenoid transition moment have been determined in the present work to be 0.82, 0.37, and 0.42 along the carotenoid triplet state magnetic axes labelled 1, 2, and 3, respectively in Fig. 4. Finally, the orientation of the primary donor and the carotenoid principal magnetic axes must be specified with respect to an external reference, e.g., the normal to the membrane. This experiment was performed by Frank et al. [22] on oriented chromatophores of *Rps. sphaeroides* wild type. The projections of the principal magnetic axes onto the normal to the membrane were found to be 0.00, 0.97, and 0.24 for the $x$, $y$, and $z$ axes of the primary donor and 0.20, 0.77, and 0.60 for the magnetic axes of the carotenoid labelled 1, 2 and 3. With this information the angles between the primary donor and the carotenoid magnetic axes can be obtained by generating the set of Euler matrices which satisfy Eqn. 11 for the range of values of $\gamma$ ($75 \pm 8°$) derived from the magneto-photoselection experiments. The projections onto the normal to the membrane help to constrain the solution set of matrices which describe the orientation between the primary donor and carotenoid principal magnetic axis systems. The Euler matrices which satisfy Eqn. 11 give the direction cosines of the angles between the carotenoid and the primary donor magnetic axes. These angles, $\theta_{ij}$, between the magnetic axes of the carotenoid and the primary donor are presented in Table III. The orientation between the primary donor and the carotenoid axis systems and their respective transition moments is shown in Fig. 4.

Magnetophotoselection experiments on *Rps. sphaeroides* wild type have revealed the orientations of the carotenoid transition moment at 514 nm and the primary donor transition moment at 870 nm with respect to the carotenoid principal magnetic axes (see Table II). These determinations have allowed the calculation of the orientation between the carotenoid and the primary donor transition moments. This angle was found to be $75 \pm 8°$. Finally, from a knowledge of the angle between the two transition moments and the angles between the magnetic axes of the primary donor and the carotenoid and the normal to the membrane [22], the angles between the primary donor and the carotenoid principal magnetic axes have been calculated (see Table III).

TABLE III

REGIONS OF SOLUTION FOR THE ANGLES BETWEEN THE CAROTENOID AND THE PRIMARY DONOR PRINCIPAL MAGNETIC AXES

The angles, $\theta_{ij}$, between the principal magnetic axes are obtained from the Euler matrices which satisfy Eqn. 11. The index $i$ references the $x$, $y$ and $z$ magnetic axes of the primary donor and $j$ references the 1, 2 and 3 magnetic axes of the carotenoid in Fig. 4

| | | |
|---|---|---|
| $75° < \theta_{x1} < 90°$ | $54° < \theta_{x2} < 63°$ | $39° < \theta_{x3} < 50°$ |
| $88° < \theta_{y1} < 90°$ | $39° < \theta_{y2} < 43°$ | $41° < \theta_{y3} < 44°$ |
| $23° < \theta_{z1} < 44°$ | $65° < \theta_{z2} < 71°$ | $69° < \theta_{z3} < 86°$ |

## Acknowledgements

The authors wish to thank Professor Douglas Hamilton for the half wave plate used in the experiments. This research is supported by a grant from the National Science Foundation (PCM-8201746).

## References

1 McGlynn, S.P., Azumi, T. and Kinoshita, M. (1969) Molecular Spectroscopy of the Triplet State, p. 364, Prentice-Hall, Englewood Cliffs, NJ
2 Kottis, P and Lefebvre, R. (1964) J. Chem. Phys. 41, 3660–3661
3 Rabold, G P. and Piette, L.H. (1966) Photochem. Photobiol 5, 733–738
4 Siegel, S and Goldstein, L (1965) J Chem. Phys. 43, 4185–4187
5 Siegel, S and Goldstein, L. (1966) J. Chem Phys. 44, 2780–2785
6 Siegel, S and Goldstein, L. (1966) J Chem. Phys. 45, 1860
7 Lhoste, J.-M , Huag, A. and Ptak, M (1966) J. Chem Phys. 44, 648–654

8 Lhoste, J -M., Huag, A. and Ptak, M. (1966) J. Chem. Phys 44, 654–657
9 El-Sayed, M.A. and Siegel, S. (1966) J. Chem Phys 44, 1416–1423
10 Clements, R.F and Sharnoff, M. (1970) Chem. Phys Lett. 7, 4–6
11 Thurnauer, M C and Norris, J.R. (1977) Chem. Phys. Lett. 47, 100–105
12 Thurnauer, M.C and Norris, J.R. (1976) Biochem. Biophys. Res. Commun. 73, 501–506
13 Frank, H A., Bolt, J., Friesner, R. and Sauer, K. (1979) Biochim Biophys. Acta. 547, 502–511
14 Trosper, T.L., Frank, H.A., Norris, J.R and Thurnauer, M.C. (1982) Biochim. Biophys. Acta 679, 44–50
15 Boxer, S.G. and Roelofs, M G. (1979) Proc. Natl. Acad. Sci. USA 76, 5636–5640
16 Vermeglio, A., Breton, J , Paillotin, G and Cogdell, R. (1978) Biochim. Biophys. Acta 501, 514–530
17 Vermeglio, A. and Clayton, R.K. (1976) Biochim. Biophys. Acta 449, 500–515
18 Paillotin, G., Vermeglio, A. and Breton, J. (1979) Biochim. Biophys. Acta 545, 249–264
19 Shuvalov, V.A. and Asadov, A.A (1979) Biochim. Biophys. Acta 545, 296–308
20 Clayton, R.K., Rafferty, C.N and Vermeglio, A. (1979) Biochim Biophys. Acta 545, 58–68
21 Breton, J and Vermeglio, A. (1982) In Photosynthesis, Vol. 1, (Govindjee, ed.), pp. 153–194, Academic Press, New York
22 Frank, H.A., Machnicki, J.P. and Toppo, P. (1984) Photochem. Photobiol. 39, 429–432
23 Frank, H.A., Friesner, R., Nairn, J.A., Dismukes, C and Sauer, K. (1979) Biochim. Biophys. Acta 547, 484–501
24 Parson, W W. and Monger, T.G. (1976) Brookhaven Symp. Biol 28, 195–212